CALENDAR-AWARE PHOTOVOLTAIC– BATTERY ASSESSMENT FOR TWELVE TEACHING ROOMS AT A SAHELIAN UNIVERSITY CAMPUS.

***Abstract*: Background:** Photovoltaic–battery planning for university campuses must account for lecture schedules, cooling demand and vacation periods, which shape both the timing and the magnitude of electricity use. When metered consumption records are unavailable, equipment inventories and annual energy balances alone cannot establish whether solar generation coincides with demand or how much storage is needed. A chronological assessment is therefore necessary to compare energy coverage, backup requirements and surplus generation. This study examines how academic calendars, differences between weather years and combined operating losses affect these trade-offs for twelve teaching rooms at a Sahelian university campus.

Methods: For twelve teaching rooms in Maradi, Niger, inventory-based demand was combined with hourly solar-model outputs for 2022 and 2023. Three calendar scenarios and finite battery energy and power limits were compared using native-time reconstruction, with separate 2023 timing diagnostics. Joint tests combined lower conversion efficiency and auxiliary demand, with additional scenarios incorporating either reduced usable battery energy or declared cleaning schedules.

Results: At constant inventory, schedule refinement reduces the non-leap demand envelope from 280.6 to 195.7 MWh; closing ordinary teaching in July–August gives 161.1 MWh in 2023. For 175 kWp, 400 kWh of usable storage and a 100 kW battery power limit at 15° south, minimum coverage under the permissive calendar is 97.9% in 2022 and 99.1% in 2023. The July–August closure raises these values to 99.7% and 99.4%. With 90% conversion efficiency in each direction and a continuous 1 kW auxiliary load, the two-year minimum under the July–August closure is 98.6% at 175 kWp and 99.5% at 200 kWp. The temporal representation of solar data also affects energy flows, although most sampled capacity thresholds are unchanged.

Key words:- Academic calendar Demand reconstruction PV–battery systems Timestamp convention Energy trade-offs Solar coverage Sahel.

Conclusion: Calendar assumptions, weather-year differences and combined operating losses materially affect candidate margins. The results support conditional energy comparisons, not an economic optimum or guaranteed autonomous operation.Nomenclature

Principal quantities

Symbol	Meaning	Unit
C_{PV}	PV nameplate capacity	kWp
$P_{PV,k}$; $P_{L,k}$	PV output and room demand at interval k	kW
E_u; E_{nom}	Usable battery energy; nominal equivalent $E_u/0.80$	kWh
P_{bat}	Equal AC charge/discharge limit	kW
E_{bak}; $E_{sur,res}$	Residual backup; residual surplus	kWh
γ; φ	Room-energy coverage; useful delivery / PV output	–
H1; H0; H2	Reference native-linear; clock-hour; native-centered support	labels
M3; M4; M5	Permissive; August closure; July–August closure	labels

1. Introduction:-

Campus photovoltaic (PV) planning requires an explicit definition of the buildings, equipment and activity periods to be supplied. Gui et al. [1] examined academic-calendar effects using monitored university buildings. Bottom-up reconstruction [2] and load forecasting for PV–battery sizing [3] address

UNDER PEER REVIEW IN IJAR

different evidence levels: an inventory-based envelope describes allowable use, whereas a calibrated demand model seeks to reproduce actual operation.

Campus planning studies couple equipment size and operation under uncertainty [4] or include economic and environmental objectives [5]. REopt [6] and multi-stage campus planning [7] further illustrate the dependence of resource decisions on service and cost assumptions. The present study separates energy coverage, residual backup, surplus, PV capacity and battery resources without assigning a monetary objective.

Temporal resolution affects PV–battery assessment [8,9]. Radiation products also differ in their sampling conventions and validation domains: SARAH-3 (labeled SARAH3 in PVGIS) is documented by Pfeifroth et al. [10], while Carpentieri et al. [11] examine time-scale-dependent satellite errors. Self-consumption, useful delivery and demand coverage require distinct denominators [12]. Degradation-aware resource planning [13] adds lifecycle effects beyond a constant-efficiency energy balance.

The regional context motivates a separate examination of maintenance assumptions. Research on dust soiling in decentralized West African solar systems [14] identifies soiling as a relevant issue for regional PV assessment. In this study, cleaning-related coefficients are declared scenario inputs; regional loss percentages are not transferred to Maradi.

Three research questions structure the work. RQ1 asks how calendar detail changes demand at a fixed equipment inventory. RQ2 asks how temporal representation and finite storage affect energy delivery. RQ3 asks how candidate margins change with vacation assumptions, weather year and combined operating losses at a fixed array geometry. The contribution is a reproducible sequence linking these questions within one service boundary. The numerical capacities remain site- and scenario-specific.

2. Study boundary and input data:-

2.1. Site, inventory and reference capacity

The study concerns twelve dedicated teaching rooms at a university campus in Maradi, Niger (13.491884° N, 7.138336° E). The whole-faculty inventory includes these rooms, eight dual-use laboratories, two computer rooms, offices and the deanery. Excluding two confirmed socket/computer duplicates leaves 178 contributing records out of 180 original entries. R1 denotes the reconciled inventory-reference balance, not measured annual consumption.

Table 1. Reconciled whole-faculty inventory-reference balance R1.

Functional group	Assigned power (kW)	Reference-day energy (kWh)
Twelve teaching rooms	110.640	892.140
Office block	128.110	965.280
Deanery	22.880	137.762
Two computer rooms	16.560	132.840
Eight laboratories	179.955	1,425.240
Total R1	458.145	3,553.262

Full arithmetic precision is retained in R1 for reconciliation. Ratings and reference durations are assigned inputs; their precision does not imply metering accuracy, and they are not coincident peak measurements.

The 351 kWp reference originates from a preliminary proposal of 520 modules rated at 675 Wp. It is a capacity benchmark, not an optimized or electrically approved installation. The twelve rooms account for about 25.1% of the reference-day energy in R1; this is not their established share of annual faculty consumption. Offices and laboratories have different, incompletely documented calendars and are excluded from this chronological boundary.

Backup denotes room demand not supplied by PV and storage; surplus denotes available generation not used within the boundary. With an available external supply, backup could become imported energy.

UNDER PEER REVIEW IN IJAR

During an outage, the same deficit would represent unmet demand unless another source intervenes. Campus outage logs, feeder details, export permission and tariffs are unavailable, so no local outage frequency or monetary value of storage is assigned.

2.2. Activity windows and calendar scenarios

The assigned daytime power is 108.300 kW: 31.920 kW for lighting, fans, laptops and projectors, and 76.380 kW for cooling. Exterior lighting adds 2.340 kW between 19:00 and 06:00, or 25.740 kWh per night. Cooling windows are shorter than lecture windows. September assessments permit all daytime equipment for four hours daily; this is the full-equipment scenario actually dispatched.

Table 2. Activity windows and dated calendar definitions.

Item	Definition
Weekday lectures / cooling	Lectures 08:00–12:00 and 15:00–18:00; cooling 09:00–12:00 and 15:00–18:00.
Saturday lectures / cooling	Lectures 08:00–12:00; cooling 09:00–12:00.
Assessments	Two Monday–Saturday weeks in September; 09:00–11:00 and 15:30–17:30; twelve dates.
M3	All ordinary slots outside September; permissive high-use comparator, including July–August.
M4	M3 with ordinary August teaching switched off.
M5	M3 with ordinary July and August teaching switched off; exterior lighting retained.
2022 examination placements	E1: 5–17 September; E2: 12–24 September; Sundays excluded.
2023 examination placements	E1: 4–16; E2: 11–23; E3: 18–30 September; Sundays excluded.

M5 represents a full-month implementation of the reported July–August vacation period, not a recovered historical timetable. M3 remains useful as a high-use comparison, and M4 tests a shorter closure. The progressive October restart, holidays and actual room assignments remain unresolved. Each year uses all pairs of consecutive complete Monday–Saturday examination weeks wholly contained in September: two placements in 2022 and three in 2023. Thus, there are six dated calendars in 2022 and nine in 2023. For example, M3_E2 means the M3 family with that year's second examination placement.

Existing 2018 field observations and their instrument details are retained in Supplement S2. They are not used to calibrate annual production or cooling demand. The original values and the distinction between incomplete secondary transcription and unavailable observations are preserved.

3. Materials and Methods:-

3.1. Demand accounting and energy screening

For each inventory entry i, the count N_i, assigned unit power p_i in watts, reference duration h_i and inclusion flag a_i give:

$$E_{R1} = \frac{\sum_i a_i N_i p_i h_i}{1000} \quad (1)$$

Independent half-hour masks M_N, M_A and M_O identify non-cooling daytime use, cooling and exterior lighting. Intervals are half-open, and $\Delta t = 0.5$ h:

$$P_{L,k} = 31.920\, M_{N,k} + 76.380\, M_{A,k} + 2.340\, M_{O,k} \quad (2)$$

The coarser comparison uses M0 (eight hours per day, Monday to Saturday), M1 (lecture slots for all daytime equipment), M2 (separate cooling), M3 (September assessment replacement) and M4 (August closure). Their annual envelopes are maximized over the seven possible starting weekdays of a non-leap year:

UNDER PEER REVIEW IN IJAR

$$E_L^{max} = \max_{j=1,\ldots,7} \sum_k P_{L,k,j}\,\Delta t \tag{3}$$

For the energy E_{use} usefully delivered to the room loads, excluding exports and storage losses, conservation provides a necessary bound:

$$\varphi = \frac{E_{use}}{E_{PV}} \le \min\left(1, \frac{E_L^{max}}{E_{PV}}\right) \tag{4}$$

Dated dispatch uses PVGIS outputs, without a second application of a global performance factor or an ambient-temperature correction. PVWatts and module-temperature models distinguish ambient and operating-cell temperatures [15,16]. The preliminary monthly accounting and the corresponding annual bounds are retained in Supplement S3.

3.2. PV resource and time representation

Twelve archived PVGIS 5.3 inputs combine SARAH3 or ERA5 radiation, 14% or 20% aggregate system loss, and three fixed geometries: 15° south, 30° south and 15° southeast [17–21]. The horizontal-plane tilt and PVGIS azimuth conventions are retained. The two radiation branches share ERA5 meteorology and the PVGIS conversion model. The source records contain hourly output for 2022–2023; the separate climate-average calculation covers 2005–2023.

PV capacities of 75, 100, 125, 150, 175, 200, 225, 250, 275, 300, 325 and 351 kWp are compared by scaling the same post-loss power profile:

$$P_{PV,k}\left(C_{PV}\right) = \frac{C_{PV}}{351}\,P_{PV,k}\left(351\right) \tag{5}$$

This energy-level scaling holds the specific yield and temporal shape constant. Inverter clipping, part-load performance and string design are outside the scope of this scaling model.

Table 3. Reference reconstruction and temporal sensitivities.

Code	SARAH3 treatment	ERA5 treatment
H1: reference	Linear interpolation through native HH:07 samples; exact half-hour integration.	Hourly means held over their clock hour.
H0: comparison	Value held over its containing clock hour.	Same as H1.
H2: sensitivity	Constant one-hour supports centered at native samples; exact overlap integration.	Same as H1.

H1 is the reference numerical reconstruction because it preserves the native sample times. H0 tests the representative-hour convention, and H2 tests a different support. None of these reconstructions supplies measured intra-hour variability. For each interval:

$$P_{PV,k}^{H} = \frac{1}{\Delta t}\int_{t_k}^{t_k+\Delta t} p^H(t)\,dt \tag{6}$$

The local year uses UTC+01:00. All 2023 boundaries are bracketed by archived records. The civil year 2022 begins at 23:00 UTC on 31 December 2021, before the start of the archive. For this missing nocturnal support only, the two corresponding closing-night native samples of 2022 are shifted back one year as an explicit periodic extension. Both are zero in all twelve inputs, as are the opening-night samples. This boundary convention is logged; it is not an acquisition of 2021 meteorology. No daytime sample is inserted or changed. Details and boundary tests are given in Supplement S4.

UNDER PEER REVIEW IN IJAR

The two-year design grid uses H1. The complete H0/H2 design comparisons are restricted to the 2023 M3/M4 inputs; their role is diagnostic. The M5 and 2022 capacity filters are not repeated under all three representations.

For the zero-valued nighttime boundaries and uniform source spacing used here, the reconstructed annual integrals coincide algebraically. Numerical equality is checked as an implementation invariant, not used as physical validation.

3.3. Battery dispatch and service metrics

At a common AC accounting bus, direct PV service and pre-storage surplus are:

$$P_{dir,k} = \min\left(P_{PV,k},\ P_{L,k}\right);\quad P_{sur,0,k} = P_{PV,k} - P_{dir,k} \tag{7}$$

The pre-storage deficit is $P_{bak,0,k} = P_{L,k} - P_{dir,k}$. A generic battery state x is measured above the protected minimum. The usable window E_u equals 80% of the nominal equivalent, corresponding to a 10–90% state-of-charge range. Detailed battery models may additionally describe thermal behavior, degradation and power-dependent efficiency [22,23].

Table 4. Main battery grid and operating assumptions.

Parameter	Values
Usable energy	25, 50, 100, 200, 400 and 800 kWh; zero-storage control.
Equal AC charge/discharge limit	25, 50, 100 and 125 kW, varied independently of energy.
Main efficiency	95% each way; 90.25% round trip.
Dispatch	PV to rooms first, then surplus charging; discharge on residual demand. No grid charging or battery export.
Annual state	Periodic state solved independently for each scenario.
Admissibility	Exploratory energy–power pairs; chemistry, BMS, thermal limits and converter suitability not established.

The charge, discharge and state equations are:

$$P_{ch,k} = \min\left(P_{sur,0,k},\ P_{ch}^{\max},\ \frac{E_u - x_k}{\eta_{ch}\,\Delta t}\right) \tag{8}$$

$$P_{dis,k} = \min\left(P_{bak,0,k},\ P_{dis}^{\max},\ \frac{\eta_{dis}\,x_k}{\Delta t}\right) \tag{9}$$

$$x_{k+1} = x_k + \eta_{ch}\,P_{ch,k}\,\Delta t - \frac{P_{dis,k}\,\Delta t}{\eta_{dis}} \tag{10}$$

Because surplus and deficit cannot coexist, simultaneous charging and discharging does not occur. The state map is iterated, with a fallback bracketed root search, until the annual state change is below 10^{-7} kWh. This eliminates a net credit from initial stored energy. Integrated balances are:

$$E_{PV} = E_{dir} + E_{ch} + E_{sur,res};\quad E_L = E_{dir} + E_{dis} + E_{bak} \tag{11}$$

The global check is $E_{PV} + E_{bak} = E_L + E_{sur,res} + E_{loss} + \Delta x$. Monthly balances retain their own state changes. Coverage of room demand and useful PV delivery are:

$$\gamma = \frac{E_{dir} + E_{dis}}{E_L};\quad \varphi = \frac{E_{dir} + E_{dis}}{E_{PV}} \tag{12}$$

UNDER PEER REVIEW IN IJAR

Annual energy coverage is distinguished from backup hours and peak backup power. A separate power-only lower bound is:

$$E_{bak} \geq \sum_{k} \max\left(0,\ P_{bak,0,k} - P_{dis}^{\max}\right) \Delta t \tag{13}$$

Throughput is reported as discharged internal energy divided by usable energy and, alternatively, by the nominal equivalent. These are accounting equivalents, not a rainflow cycle count or a life prediction. The ratio P_{bat}/E_{nom} is flagged for product checking: for 25 kWh usable and 125 kW it is 4 h^{-1} at the AC bus, rather than a verified cell-level C-rate. No commercial feasibility claim is made for these exploratory extremes.

3.4. Geometry-specific comparison and calendar/year tests

For each fixed geometry, H1 is evaluated over both radiation sources, both loss inputs, all applicable examination placements and the full PV/battery grid. This gives 21,600 balances for 2022 and 32,400 for 2023, including zero-storage controls. The 21,600 overlapping 2023 M3/M4 balances reproduce the archived H1 results. The M5 and 2022 calculations are extensions, not relabeled earlier outputs.

Coverage filters are evaluated separately by year and calendar family, then jointly across the two years when explicitly stated:

$$\gamma_{\min}(g,H) = \min_{s \in S_g} \gamma(g,H,s) \tag{14}$$

Targets of 95%, 98% and 99% are illustrative energy filters. Passing grid points identify the smallest sampled capacity under specified assumptions; they do not locate a continuous optimum. Unrounded values determine whether a filter is passed; displayed values are rounded for readability. Paired 175-versus-200 kWp comparisons use identical source, loss and calendar inputs. A further 1,080 candidate calculations impose the same 2023 activity sequence on both weather years, separating weather-profile changes from weekday placement.

To show dependence on the dominant load, cooling alone is multiplied by 0.50, 0.75 or 1.00 during its permitted slots. The 4,320 additional lower-cooling cases use 400 kWh/100 kW over the full PV grid. Their ranges are scenario envelopes, not estimated confidence intervals. The temperature-indexed alternative and its uncalibrated status are documented in the supplement.

3.5. Combined operating and cleaning sensitivities

Five candidate triplets are tested: 175/400/100, 200/400/100, 250/400/100, 150/800/100 and 275/200/100 (PV kWp / usable kWh / battery kW). J1 combines 90% efficiency in each direction with a continuous auxiliary demand of 2 W per original nominal-equivalent kWh. At 400 kWh usable, this is 1 kW. J2 additionally reduces available usable energy by 20%, without claiming a measured state of health. Auxiliaries remain tied to the original nominal equivalent.

Dispatch serves room-plus-auxiliary demand. Remaining deficits are allocated proportionally to simultaneous room and auxiliary loads, and only room delivery enters room coverage. Auxiliary levels are declared stress assumptions because no standby or thermal-management measurements are available for a selected product.

The cleaning scenarios replace, rather than blindly add to, a soiling component within the aggregate PV loss. An embedded reference soiling fraction $s_0 = 0.02$ is explicitly assumed for this decomposition. Other losses satisfy $(1 - L_{other})(1 - s_0) = 1 - L_{archive}$. A surface-loss scenario s(t) therefore gives:

$$P_{PV,k}^{soil} = P_{PV,k}^{archive} \times \frac{1 - s_k}{1 - s_0} \tag{15}$$

Soiling loss increases by 0.20 percentage points per day in November–April, 0.10 in May–June and October, and 0.05 in July–September; cleaning every 15, 30 or 60 days resets the loss to zero. Cleaning

UNDER PEER REVIEW IN IJAR

starts on 1 January, a 20% cap is imposed, and no rainfall reset is inferred. These rates, intervals and the 2% decomposition are analytical assumptions, not Maradi measurements. Separate cleaning cases and cleaning combined with J1 are evaluated. The 7,200 resulting rows include 900 baseline repetitions and 6,300 altered scenarios.

4. Results:-

4.1. Calendar-dependent demand

Table 5. Demand envelopes and dated scenario energy.

Calendar	2022 (MWh)	2023 (MWh)
M0 envelope	280.58	280.58
M1 envelope	229.79	229.79
M2 envelope	205.88	205.88
M3 dated demand	194.33	194.30
M4 dated demand	177.22	177.19
M5 dated demand	161.12	161.09

M0–M2 are seven-alignment non-leap envelopes, repeated here for comparison; dated M3–M5 use each year's weekdays. The M3 and M4 envelopes remain 195.659 and 178.552 MWh, respectively.

Resolving lecture, cooling and assessment timing reduces the fixed-inventory envelope from 280.58 to 195.66 MWh (−30.27%). In 2023, M3, M4 and M5 require 194.30, 177.19 and 161.09 MWh, respectively. In 2022, their values are 194.33, 177.22 and 161.12 MWh. These differences arise from modeled use and weekday placement, not measured savings. Full-power cooling represents 123.96 MWh, or about 63.8% of M3 demand.

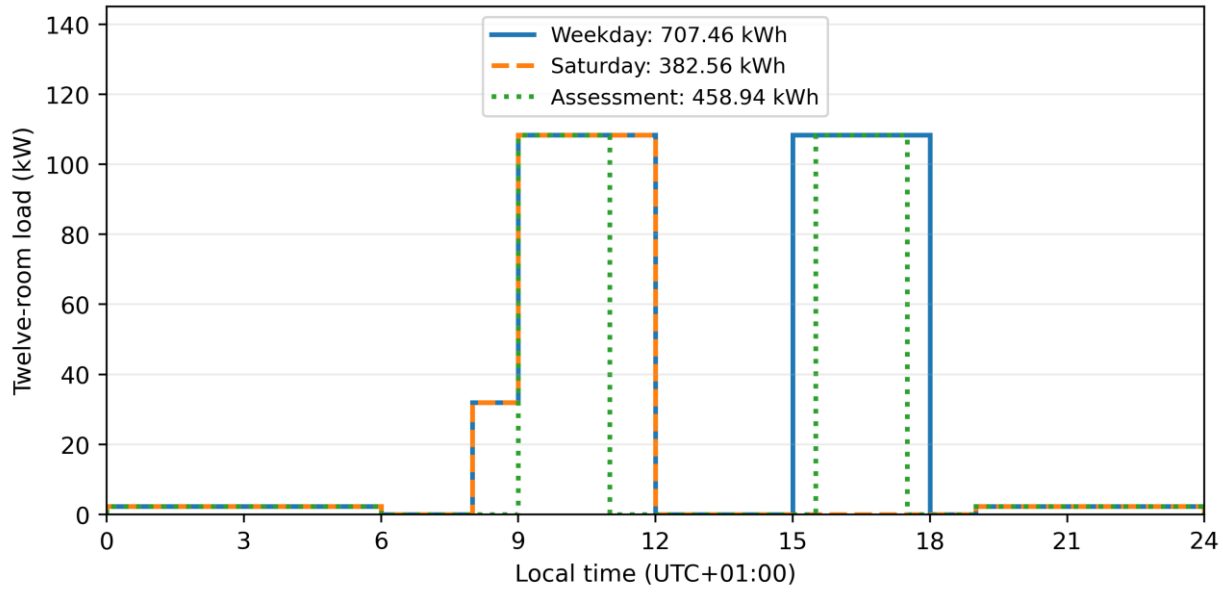


Figure 1. Daily demand profiles used in the dispatch, including independent exterior lighting. Assessment demand reaches 108.3 kW; the Saturday profile is shown separately.

4.2. Temporal representation and storage

The archived climate-average 351 kWp production spans 570.38–635.40 MWh/year, giving an M3 ideal useful-delivery ceiling of 30.79–34.30%. The corresponding dated 2023 production is 570.42–633.66 MWh. Annual resource adequacy and coincident room service are different tests.

UNDER PEER REVIEW IN IJAR

Table 6. 2023 no-storage comparison at 351 kWp, 15° south, 14% losses, M3_E2.

Input	PV (MWh)	Direct (MWh)	Backup (MWh)	Coverage (%)
SARAH3 H0	633.66	169.92	24.37	87.46
SARAH3 H1	633.66	163.13	31.17	83.96
SARAH3 H2	633.66	161.93	32.37	83.34
ERA5 H0/H1/H2	627.30	162.95	31.34	83.87

At equal annual SARAH3 energy, H1 gives about 3.5 percentage points less direct coverage than H0 in this reference. Its time support shifts the afternoon energy available during occupied intervals. This is a numerical representation effect; it does not establish which trace matches measured subhourly power.

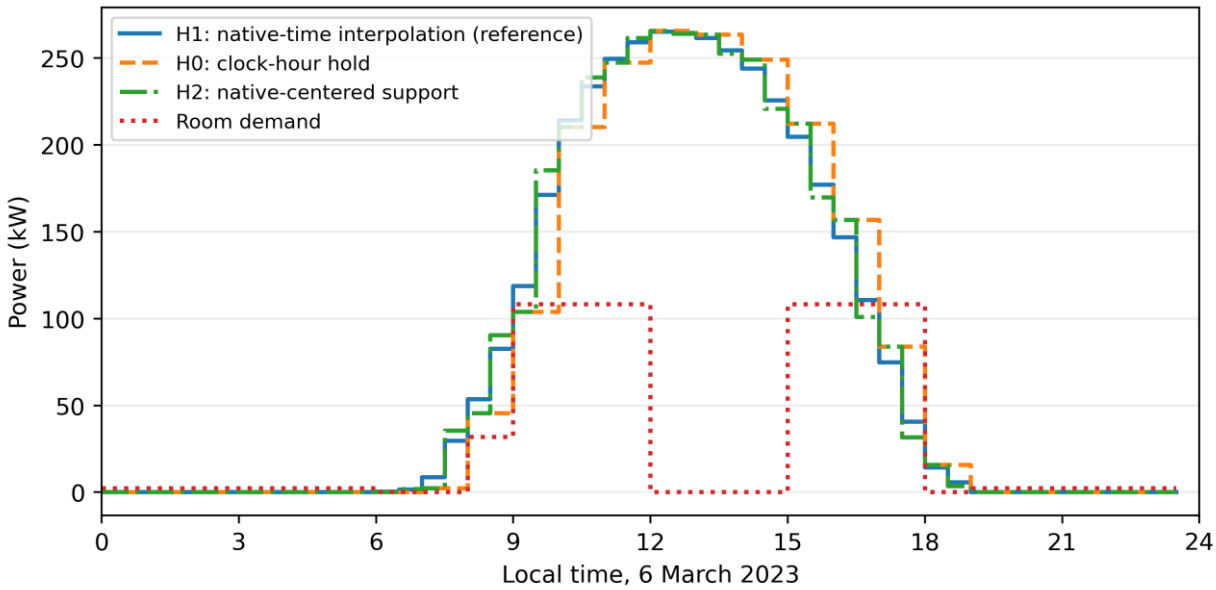


Figure 2. Alternative supports of the same hourly source data on 6 March 2023. H1 is the analysis reference; the lines do not represent measured subhourly production.

Table 7. Storage comparison for the same 2023 SARAH3 reference.

Usable kWh / kW	H0 backup (MWh)	H1 backup (MWh)	H1 coverage (%)	H1 loss (MWh)
0/0	24.3722	31.1653	83.96	0.000
100/100	2.3348	4.5276	97.67	2.878
200/100	0.7857	0.8464	99.56	3.275
400/100	0.0230	0.0270	99.99	3.364
400/125	0.0024	0.0119	99.99	3.366
800/125	0.0000	0.0000	100.00	3.367

Residual energy is reported finely enough to distinguish near-complete from complete coverage. For example, H1 at 400 kWh/100 kW still requires 26.95 kWh of backup.

The timing effect is not restricted to zero storage: at 100 kWh/100 kW, backup changes from 2.335 MWh in H0 to 4.528 MWh in H1. For the nine 2023 M3 combinations of three array geometries and usable storage capacities of 200, 400 and 800 kWh at a 100 kW battery power limit, the smallest sampled PV capacity satisfying the 99% coverage filter is unchanged across H0, H1 and H2. In the complete archived set of 450 method-comparable filters, H0 and H1 select the same sampled capacities and H2 changes four. Energy-flow sensitivity therefore does not imply that every discrete capacity decision changes.

UNDER PEER REVIEW

4.3. PV reduction and storage throughput

Table 8. PV reduction at 400 kWh/100 kW, H1 reference, 2023 M3_E2.

PV (kWp)	Coverage (%)	Backup (MWh)	Surplus (MWh)	Usable-window cycles
351	99.99	0.027	436.03	81.9
250	99.95	0.104	252.61	110.1
200	99.69	0.611	161.61	140.3
175	99.45	1.070	115.94	164.8
150	98.06	3.777	72.31	194.0

Reducing PV from 351 to 175 kWp lowers reference surplus from 436.0 to 115.9 MWh but raises backup and battery throughput. Internal discharge corresponds to about 82 usable-window cycles at 351 kWp and 165 at 175 kWp (about 66 and 132 nominal-energy equivalents). This change raises a lifecycle question; it is not a quantified degradation or replacement forecast.

4.4. Weather-year and vacation effects on capacity filters

Table 9. Smallest sampled PV capacity passing the 99% filter at 400 kWh/100 kW under H1.

Fixed geometry	Year	M3 (kWp)	M4 (kWp)	M5 (kWp)
15° south	2022	225	200	175
15° south	2023	175	175	175
30° south	2022	225	200	200
30° south	2023	200	200	200
15° southeast	2022	225	200	175
15° southeast	2023	200	175	175

Each entry is based on the minimum coverage across both radiation sources, both loss inputs and that year's examination placements. Full battery-grid results and 95/98/99% filters are supplied in the supplement and the numerical files.

At 15° south, the M3 filter changes from 175 kWp in 2023 to 225 kWp in 2022. Closing August reduces the 2022 value to 200 kWp, while closing July–August reduces it to 175 kWp. The two years therefore do not support a universal 175 kWp selection for permissive use. The vacation scenario changes the requested service, not the equipment efficiency.

Table 10. Candidate margins at 15° south and 400 kWh/100 kW.

PV (kWp)	Calendar	2022 min. (%)	2023 min. (%)	Max. backup (MWh)	Max. peak (kW)
175	M3	97.88	99.09	4.128	102.9
175	M5	99.67	99.42	0.938	101.8
200	M3	98.96	99.58	2.024	102.1
200	M5	99.95	99.75	0.408	94.3
250	M3	99.58	99.87	0.824	100.6
250	M5	99.98	99.90	0.158	90.8

The 175 and 200 kWp designs have different modeled performance under paired inputs. These differences do not constitute a validated procurement ranking, but neither do they establish equivalence. The retained files provide paired differences rather than differences between unrelated extrema. In the fixed-2023-calendar sensitivity, the 175 kWp M3 minimum is 97.24% with 2022 weather and 99.09% with 2023 weather: weekday changes alone do not explain the year effect.

UNDER PEER REVIEW IN IJAR

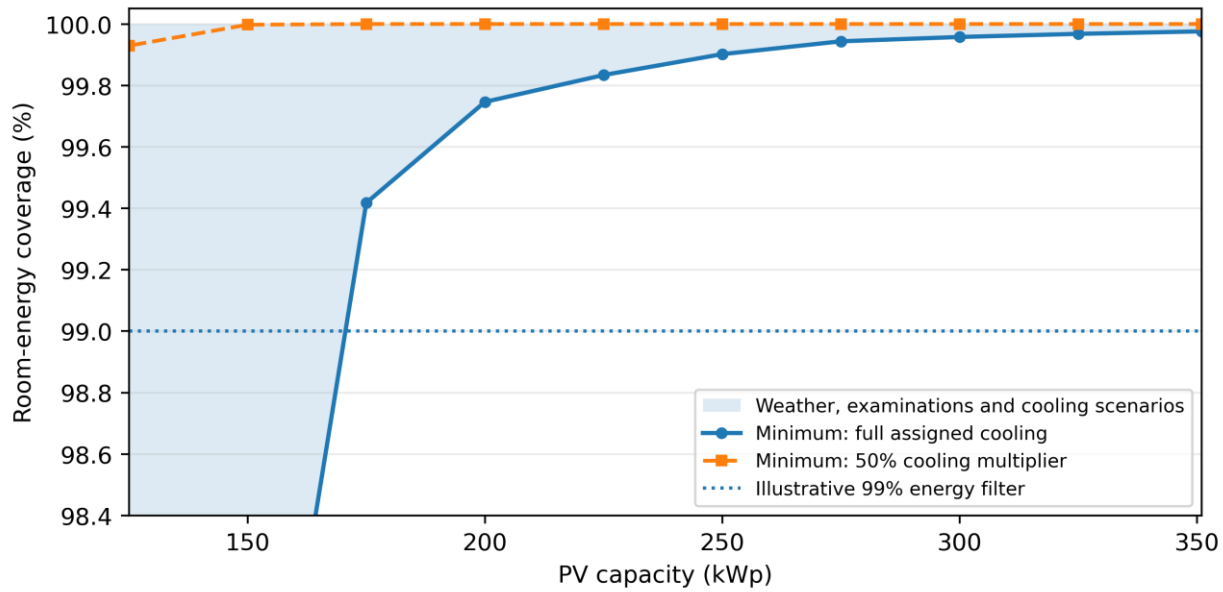


Figure 3. Zoom near the 99% filter for 15° south, M5 and 400 kWh/100 kW. The shaded range spans the two weather years, source/loss inputs, examination placements and declared cooling multipliers. It is a scenario range, not a confidence interval; markers denote simulated capacities. A full-range view is provided in the supplement.

4.5. Which dates produce the residual deficit?

Table 11. Limiting periods for the 175/400/100 SARAH3/15° south/14%/E2 trace.

Year	Calendar	Annual backup (MWh)	Month with highest backup energy	Day with highest backup energy	Day backup (kWh)
2022	M3	2.726	August	2022-08-19	458.3
2022	M4	0.950	July	2022-07-28	290.5
2022	M5	0.175	June	2022-06-11	45.4
2023	M3	1.070	August	2023-03-21	239.1
2023	M4	0.578	March	2023-03-21	239.1
2023	M5	0.578	March	2023-03-21	239.1

Note: The month with the highest cumulative backup energy need not contain the day with the highest daily backup energy, because monthly totals and daily maxima are different indicators.

For the 2022 reference, August and July dominate M3 backup. Their removal changes the critical period to June, rather than merely reducing the annual total. In 2023, 21 March remains the largest deficit day under M5, so vacation closure does not remove all demanding periods. The five largest-deficit dates for every tested candidate, source and calendar are retained in the result files; the table illustrates one declared reference case and does not identify universal worst dates.

UNDER PEER REVIEW

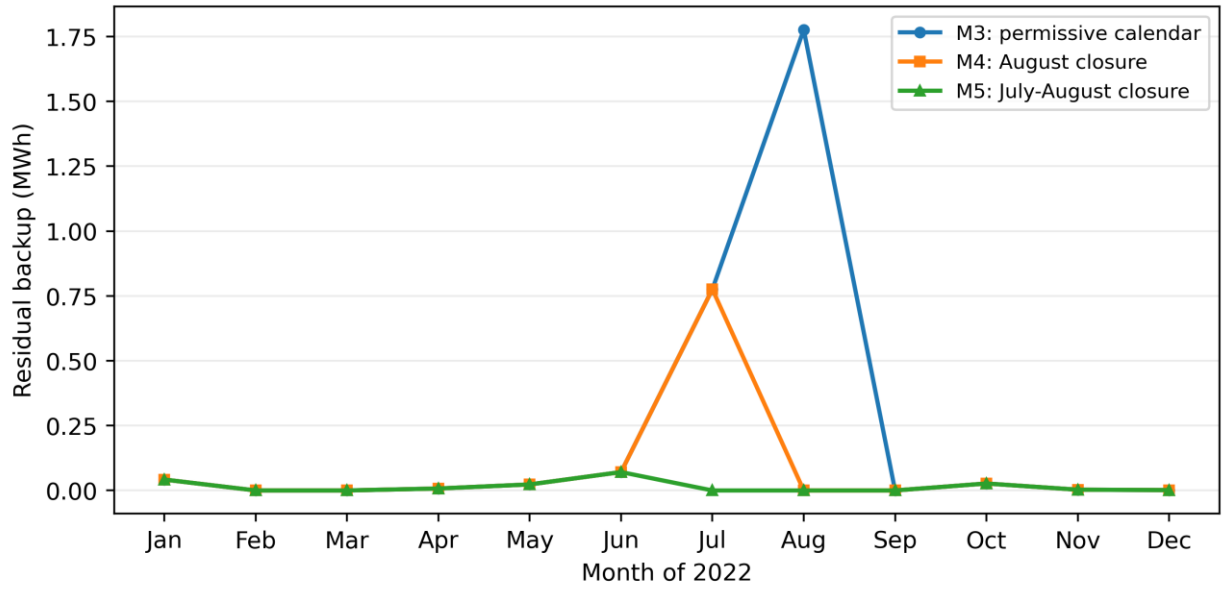


Figure 4. Monthly backup for the 2022 reference candidate. The separate vacation assumptions reveal how allowing ordinary July–August use can influence a capacity comparison.

4.6. Combined storage and cleaning conditions

Table 12. Two-year minimum room coverage for M5, 15° south, 400 kWh/100 kW.

PV (kWp)	Main (%)	J1 (%)	J2 (%)	J1 + 60-day cleaning (%)
175	99.42	98.56	97.89	98.06
200	99.75	99.50	99.06	99.44
250	99.90	99.82	99.58	99.80

J1: 90% each-way efficiency plus a 1 kW continuous auxiliary load. J2: J1 plus a 20% usable-energy reduction. Cleaning replaces the assumed embedded 2% soiling component; parameters are uncalibrated.

Under M5, the two-year 175 kWp minimum falls from 99.42% to 98.56% with J1 and to 97.89% with J2. At 200 kWp, the corresponding values are 99.75%, 99.50% and 99.06%. Combined constraints therefore consume more margin than a single-factor check would suggest. Residual peak demand must still be assessed separately; under J1 at 200 kWp it can reach about 101 kW across the two years despite high annual coverage.

UNDER PEER REVIEW

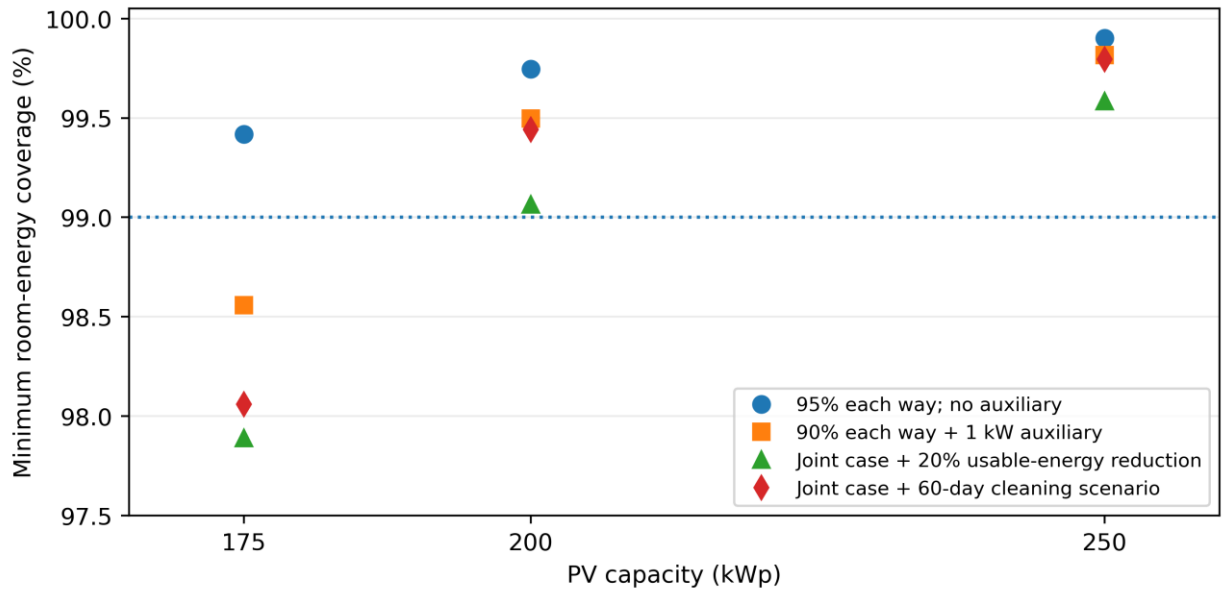


Figure 5. Discrete combined-condition comparisons at fixed geometry and nominal resource basis. Markers alone are used; no intermediate capacity is inferred.

The replacement soiling scenarios can increase or decrease production relative to the assumed 2% reference: frequent cleaning can make the modeled surface cleaner than that reference. For M5 at 15° south, the 60-day cleaning case changes the 175 kWp minimum to 99.31% by itself and to 98.06% when combined with J1. The 200 kWp joint value is 99.44%. These are conditional maintenance comparisons, not observed cleaning benefits or a measured regional dust correction.

5. Discussion:-

5.1. Transferable findings and decision relevance

The comparison separates four quantities often conflated in preliminary assessments: allowable annual demand, coincident direct service, energy that storage can shift, and residual backup power. Calendar detail changes the first quantity; time support changes coincidence; finite energy and power constrain transfer; joint losses affect the remaining margin. Holding the service boundary fixed makes these effects identifiable within the model.

A useful general lesson is to test whether the dates responsible for a candidate's deficit belong to the proposed service calendar. In the 2022 reference, permissive July–August teaching materially changes the sampled capacity filter. A second lesson is that annual energy coverage does not remove a high-power backup requirement. A third is that a threshold crossing smaller than the scenario spread is a fragile screening result, not evidence for a unique final size.

The weather-year comparison does not make 175 and 200 kWp equivalent. It shows that their different modeled margins need to be assessed under the same calendar and joint assumptions. Reduced PV can improve the fraction of generation used within the boundary while increasing battery throughput and backup. This is an energy trade-off; a least-cost ranking would require equipment prices, replacement assumptions, service priorities and export rules.

5.2. Limits and validation priorities

Room occupancy and cooling duty are reconstructed, not metered. Cooling scenario spreads are not statistical uncertainty estimates. M5 imposes a full July–August closure for ordinary use; actual transitions and the October restart remain unknown. Expanding service to laboratories or offices requires

UNDER PEER REVIEW

their own schedules and circuits. The 25.1% reference-day share cannot establish the rooms' annual share of the faculty demand.

Only two weather years are compared. The difference between them is not a long-term failure probability. The 2022 opening-night completion is explicit, and the underlying solar time series still lack measured intra-hour variability. H1 is a numerical reference, not a calibrated correction to the satellite product. The 25 kWp sampling interval, deterministic source/loss choices and fixed geometry limit the interpretation of capacity thresholds.

The battery is represented by a generic AC energy model. Joint stresses improve the screening but do not validate a product's efficiency curve, standby power, thermal-management demand, degradation or islanding functions. The cleaning rates and 2% loss decomposition are assumptions. Actual product and soiling measurements would be required to replace them. Land assessment must distinguish module area from plant footprint [24]. Field-data quality and original electrical-compatibility details are retained in Supplements S2–S3; quality-control flags alone do not identify a sensor's orientation [25].

Validation priorities are matched-circuit consumption measurements, actual room allocations, additional weather years and product-compatible electrical checks. The type and availability of backup should be characterized from campus records before valuing storage. No local outage frequency, economic optimum or procurement recommendation follows from the present scenarios.

5.3. Reproducibility

The maintained calculation package records original file hashes, calendar masks, boundary completion, parameter sets, full-precision balances and geometry-specific filters. The 54,000 H1 balances, 1,080 common-calendar checks, 4,320 cooling sensitivities and 7,200 joint/cleaning rows are stored separately, including their repeated controls. The 21,600 overlapping balances agree with the archived H1 results to within 6×10^{-11} in the reported units. Eight complete trajectories are checked against an independently coded scalar dispatch. All 248 grouped checks pass; the largest main annual energy residual is below 3.2×10^{-8} kWh. These are implementation checks. The package is maintained for access on reasonable request; no public deposit or DOI is claimed.

6. Conclusion:-

Academic timing materially changes fixed-inventory demand. The M3 annual envelope is 195.66 MWh compared with 280.58 MWh under uniform eight-hour use; the July–August closure scenario requires about 161.1 MWh in each of the two dated years. These differences represent modeled service assumptions.

Time representation changes direct solar delivery and some battery flows, but most sampled capacity filters remain unchanged. Native-time interpolation is used as the numerical reference, with other representations retained as sensitivities rather than treated as observed alternatives.

The two-year comparison changes the interpretation of narrow capacity margins. At 15° south and 400 kWh/100 kW, the permissive M3 calendar requires 225 kWp in 2022 versus 175 kWp in 2023 to pass the sampled 99% filter. Under M5, 175 kWp passes both baseline years but fails the combined efficiency/auxiliary tests. The 200 and 250 kWp cases provide different margins and surpluses, not a unique or economically ranked solution.

The principal practical requirement is to match service calendars and joint operating assumptions before interpreting a high annual coverage percentage as a design recommendation. Metering, product qualification and longer-term assessment remain necessary for installation decisions.

UNDER PEER REVIEW IN IJAR

References:-

[1] X. Gui, Z. Gou and Y. Lu, "Reducing university energy use beyond energy retrofitting: The academic calendar impacts," Energy and Buildings, 231, 110647, 2021. doi: 10.1016/j.enbuild.2020.110647.

[2] F. Lombardi, S. Balderrama, S. Quoilin and E. Colombo, "Generating high-resolution multi-energy load profiles for remote areas with an open-source stochastic model," Energy, 177, 433–444, 2019. doi: 10.1016/j.energy.2019.04.097.

[3] S. E. Eyimaya, N. Altin and A. Nasiri, "Optimization of Photovoltaic and Battery Storage Sizing in a DC Microgrid Using LSTM Networks Based on Load Forecasting," Energies, 18(14), 3676, 2025. doi: 10.3390/en18143676.

[4] M. Furukakoi, A. Nakadomari, A. Uehara, N. Krishnan, A. M. Hemeida and T. Senjyu, "Optimization of PV and battery systems in university campuses: A combined planning and operation approach under uncertainties," Energy and Buildings, 335, 115512, 2025. doi: 10.1016/j.enbuild.2025.115512.

[5] S. İşçan and O. Arıkan, "Optimizing battery energy storage system for campus micro grid: Economic and environmental benefits of strategic sizing," Journal of Energy Storage, 124, 116905, 2025. doi: 10.1016/j.est.2025.116905.

[6] D. Cutler, D. Olis, E. Elgqvist, X. Li, N. Laws, N. DiOrio, A. Walker and K. Anderson, REopt: A Platform for Energy System Integration and Optimization. NREL/TP-7A40-70022, September 2017. doi: 10.2172/1395453.

[7] A. E. Şener, B. Kocuk and T. Yüksel, "A Dynamic Strategic Plan for Transition to Campus-Scale Clean Electricity Using Multi-Stage Stochastic Programming," arXiv:2506.16423, 2025. Preprint. doi: 10.48550/arXiv.2506.16423.

[8] T. Beck, H. Kondziella, G. Huard and T. Bruckner, "Assessing the influence of the temporal resolution of electrical load and PV generation profiles on self-consumption and sizing of PV-battery systems," Applied Energy, 173, 331–342, 2016. doi: 10.1016/j.apenergy.2016.04.050.

[9] C. Rus-Casas, C. Gilabert-Torres and J. I. Fernández-Carrasco, "Optimizing Energy Management and Sizing of Photovoltaic Batteries for a Household in Granada, Spain: A Novel Approach Considering Time Resolution," Batteries, 10(10), 358, 2024. doi: 10.3390/batteries10100358. Author manuscript: arXiv:2411.00159.

[10] U. Pfeifroth, J. Drücke, S. Kothe, J. Trentmann, M. Schröder and R. Hollmann, "SARAH-3 – satellite-based climate data records of surface solar radiation," Earth System Science Data, 16, 5243–5265, 2024. doi: 10.5194/essd-16-5243-2024.

[11] A. Carpentieri, D. Folini, M. Wild, L. Vuilleumier and A. Meyer, "Satellite-derived solar radiation for intra-hour and intra-day applications: Biases and uncertainties by season and altitude," Solar Energy, 255, 274–284, 2023. doi: 10.1016/j.solener.2023.03.027.

[12] R. Luthander, J. Widén, D. Nilsson and J. Palm, "Photovoltaic self-consumption in buildings: A review," Applied Energy, 142, 80–94, 2015. doi: 10.1016/j.apenergy.2014.12.028.

[13] H. Z. Butt and X. Li, "Enhancing Optimal Microgrid Planning with Adaptive BESS Degradation Costs and PV Asset Management: An Iterative Post-Optimization Correction Framework," Electric Power Systems Research, 247, 111785, 2025. doi: 10.1016/j.epsr.2025.111785.

[14] S. Isaacs, O. Kalashnikova, M. J. Garay, A. van Donkelaar, M. S. Hammer, H. Lee and D. Wood, "Dust soiling effects on decentralized solar in West Africa," Applied Energy, 340, 120993, 2023. doi: 10.1016/j.apenergy.2023.120993.

[15] A. P. Dobos, PVWatts Version 5 Manual. NREL/TP-6A20-62641, 2014. doi: 10.2172/1158421.

[16] D. Faiman, "Assessing the outdoor operating temperature of photovoltaic modules," Progress in Photovoltaics: Research and Applications, 16(4), 307–315, 2008. doi: 10.1002/pip.813.

[17] European Commission, Joint Research Centre, "API non-interactive service," PVGIS 5 documentation. Parameter definitions and versioned PVcalc endpoint. Accessed 26 October 2026. https://joint-research-centre.ec.europa.eu/photovoltaic-geographical-information-system-pvgis/using-pvgis-5/api-non-interactive-service_en.

[18] European Commission, Joint Research Centre, "Grid-connected PV," PVGIS 5 tools. Definitions of monthly-mean daily production, monthly energy and annual outputs. Accessed 26 October 2026. https://joint-research-centre.ec.europa.eu/photovoltaic-geographical-information-system-pvgis/using-pvgis-5/pvgis-5-tools/grid-connected-pv_en.

[19] European Commission, Joint Research Centre, "Using PVGIS 5," version and dataset documentation. Accessed 26 October 2026. https://joint-research-centre.ec.europa.eu/photovoltaic-geographical-information-system-pvgis/using-pvgis-5_en.

[20] European Commission, Joint Research Centre, "Hourly radiation," PVGIS documentation. Accessed 26 October 2026. https://joint-research-centre.ec.europa.eu/photovoltaic-geographical-information-system-pvgis/using-pvgis-5/pvgis-5-tools/hourly-radiation_en.

[21] European Commission, Joint Research Centre, "PVGIS 5 user manual," Section 9.3, Note on PVGIS Data Timestamps. Accessed 26 October 2026. https://joint-research-centre.ec.europa.eu/photovoltaic-geographical-information-system-pvgis/using-pvgis-5/pvgis-5-user-manual_en.

[22] N. DiOrio, A. Dobos, S. Janzou, A. Nelson and B. Lundstrom, Technoeconomic Modeling of Battery Energy Storage in SAM. NREL/TP-6A20-64641, 2015. doi: 10.2172/1225314.

UNDER PEER REVIEW IN IJAR

[23] System Advisor Model (SAM), “Battery Storage,” online model documentation. Accessed 26 October 2026. https://samrepo.nlr.gov/help/battery_storage.html. Used for model-scope context; the present simplified controller is not a SAM run.

[24] M. Bolinger and G. Bolinger, “Land Requirements for Utility-Scale PV: An Empirical Update on Power and Energy Density,” IEEE Journal of Photovoltaics, 12(2), 589–594, 2022. doi: 10.1109/JPHOTOV.2021.3136805.

[25] C. N. Long and E. G. Dutton, “BSRN Global Network recommended QC tests, V2.0,” Baseline Surface Radiation Network, technical guide. Accessed 26 October 2026. https://bsrn.awi.de/fileadmin/user_upload/bsrn.awi.de/Publications/BSRN_recommended_QC_tests_V2.pdf.

UNDER PEER REVIEW IN IJAR